

Genomic Amplification of *CD274* (PD-L1) in Small-Cell Lung Cancer

Julie George¹, Motonobu Saito^{2,3}, Koji Tsuta⁴, Reika Iwakawa², Kouya Shiraishi², Andreas H. Scheel⁵, Shinsuke Uchida⁴, Shun-ichi Watanabe⁶, Ryo Nishikawa⁷, Masayuki Noguchi⁸, Martin Peifer⁹, Se Jin Jang¹⁰, Iver Petersen¹¹, Reinhard Büttner⁵, Curtis C. Harris¹², Jun Yokota^{2,13}, Roman K. Thomas^{1,5,14}, and Takashi Kohno^{2,15}

Abstract

Purpose: Programmed death ligand-1 (PD-L1), encoded by the *CD274* gene, is a target for immune checkpoint blockade; however, little is known about genomic *CD274* alterations. A subset of small-cell lung cancer (SCLC) exhibits increased copy number of chromosome 9p24, on which *CD274* resides; however, most SCLCs show low expression of PD-L1. We therefore examined whether *CD274* is a target of recurrent genomic alterations.

Experimental Design: We examined somatic copy number alterations in two patient cohorts by quantitative real-time PCR in 72 human SCLC cases (cohort 1) and SNP array analysis in 138 human SCLC cases (cohort 2). Whole-genome sequencing revealed the detailed genomic structure underlying focal amplification. PD-L1 expression in amplified cases from cohorts 1 and 2 was further examined by transcriptome sequencing and immunohistochemical (IHC) staining.

Results: By examining somatic copy number alterations in two cohorts of primary human SCLC specimens, we observed 9p24 copy number gains (where *CD274* resides) and focal, high-level amplification of *CD274*. We found evidence for genomic targeting of *CD274*, suggesting selection during oncogenic transformation. *CD274* amplification was caused by genomic rearrangements not affecting the open reading frame, thus leading to massively increased *CD274* transcripts and high level expression of PD-L1.

Conclusions: A subset (4/210, 1.9%) of human SCLC patient cases exhibits massive expression of PD-L1 caused by focal amplification of *CD274*. Such tumors may be particularly susceptible to immune checkpoint blockade. *Clin Cancer Res*; 23(5); 1220–6. ©2016 AACR.

¹Department of Translational Genomics, Center of Integrated Oncology Cologne-Bonn, Medical Faculty, University of Cologne, Cologne, Germany. ²Division of Genome Biology, National Cancer Center Research Institute, Tokyo, Japan. ³Department of Organ Regulatory Surgery, Fukushima Medical University School of Medicine, Fukushima, Japan. ⁴Division of Pathology and Clinical Laboratories, National Cancer Center Hospital, Tokyo, Japan. ⁵Institute of Pathology, University Hospital Cologne, Cologne, Germany. ⁶Division of Thoracic Surgery, National Cancer Center Hospital, Tokyo, Japan. ⁷Department of Neuro-Oncology/Neurosurgery, Saitama Medical University International Medical Center, Saitama, Japan. ⁸Department of Pathology, Faculty of Medicine, University of Tsukuba, Ibaraki, Japan. ⁹Center for Molecular Medicine Cologne (CMCC), University of Cologne, Cologne, Germany. ¹⁰Center for Cancer Genome Discovery, Asan Institute for Life Science, Asan Medical Center, Seoul, Korea. ¹¹Institute of Pathology, Jena University Hospital, Friedrich-Schiller-University, Jena, Germany. ¹²Laboratory of Human Carcinogenesis, Center for Cancer Research, National Cancer Institute, NIH, Bethesda, Maryland. ¹³Cancer Genome Biology Group, Institute of Predictive and Personalized Medicine of Cancer, Barcelona, Spain. ¹⁴German Cancer Research Center, German Cancer Consortium (DKTK), Heidelberg, Germany. ¹⁵Division of Translational Research Exploratory Oncology Research and Clinical Trial Center, National Cancer Center, Tokyo, Japan.

Note: Supplementary data for this article are available at Clinical Cancer Research Online (<http://clincancerres.aacrjournals.org/>).

J. George and M. Saito contributed equally to this article.

Corresponding Authors: Takashi Kohno, National Cancer Center Research Institute, 1-1 Tsukiji 5-chome, Chuo-ku, Tokyo 104-0045, Japan. Phone: 813-3547-5272; Fax: 813-3542-0807; E-mail: tkkohno@ncc.go.jp; and Roman K. Thomas, University of Cologne, 50931 Cologne, Germany. E-mail: roman.thomas@uni-koeln.de

doi: 10.1158/1078-0432.CCR-16-1069

©2016 American Association for Cancer Research.

Introduction

Small-cell lung cancer (SCLC) is the most aggressive type of lung cancer and accounts for about 15% of all lung cancer cases (1). Unfortunately, most SCLC cases are diagnosed at advanced, metastatic stage, when treatment is only palliative. Furthermore, although most SCLC tumors respond initially to chemotherapy, disease recurs quickly in all patients and is universally fatal within only few months. Beyond chemotherapy, no effective drugs have been approved over the last decades, thus necessitating novel and effective therapeutic approaches (2).

Blockade of immune checkpoints increases antitumor immunity (3, 4). Clinical trials have shown that inhibiting cytotoxic T-lymphocyte antigen 4 (CTLA-4) or the interaction between programmed death-1 (PD-1) and the PD-1 ligand, PD-L1, can overcome the intrinsic resistance to immune surveillance in various types of cancers, including lung cancer, thus leading to significant and durable clinical responses (5–8). More recently, anti-PD-1/PD-L1–based immunotherapies have also shown early signs of clinical efficacy in SCLC (9–11).

Expression of PD-L1 protein in tumor cells has been proposed as a predictive biomarker of response to anti-PD-1/PD-L1 treatment (7, 8, 12). However, the mechanisms governing levels of PD-L1 expression in tumor cells remain poorly understood and several patients respond to checkpoint blockade, whose tumors lacked expression of PD-L1. Thus, efficacy might not primarily be related to basic levels of PD-L1 expression. In addition, efficacy of PD-1 blockade segregates with mutational burden in the tumor in

Translational Relevance

Small-cell lung cancer (SCLC) is the most aggressive and lethal lung cancer subtype; yet, treatment options have not significantly changed in the past decades. Thus, novel therapeutic approaches are urgently needed. The use of immune checkpoint blockade targeting programmed death ligand-1 (PD-L1), encoded by the *CD274* gene, has shown promising early clinical activity in SCLC patients. However, most SCLC tumors lack PD-L1 expression, and little is known about the somatic mechanisms that govern response to immune checkpoint inhibition. Here, we report on a subset of SCLC tumors (1.9%, 4/210 cases) that exhibit massive expression of PD-L1 caused by focal amplification of *CD274*. Such tumors may be particularly susceptible to immune checkpoint blockade.

melanoma and lung cancer and with mutations in DNA repair genes in colorectal cancer (13).

We have recently shown that PD-L1 expression is almost universally absent in SCLC tumor cells (14). However, approximately 50% of cases exhibited PD-L1 expression in tumor-infiltrating immune cells. Although two other studies reported high expression of PD-L1 in SCLC tumor cells in the majority of the cases (15, 16), both studies had involved an antibody that has been discontinued due to lack of specificity for PD-L1. When examining PD-L1 expression by RNA sequencing, which is less prone to these methodological distortions, PD-L1 expression in SCLC is generally low to absent (14). We therefore sought to determine in detail genomic alterations that might affect the levels of PD-L1 expression in SCLC.

Patients and Methods

Patients

Between 1985 and 2013, tumor and corresponding noncancerous tissues were obtained from SCLC patients at surgery, autopsy, or biopsy with the approval of each institutional review board. Two independent cohorts were examined. Cohort 1 comprised 88 tumors from 72 patients recruited from National Cancer Center Hospital, Tokyo, Japan, Saitama Medical University, Saitama, Japan, the University of Tsukuba, Ibaraki, Japan, and hospitals in the Metropolitan Baltimore area. Sixty-two of these samples had been previously subjected to genome scanning (17). Cohort 2 comprised 138 tumors from 138 SCLC patients diagnosed with stage I-IV SCLC. These tumor samples are enriched for Caucasian ethnicity and were collected by multiple collaborating centers. Cohort 2 cases were previously analyzed in genomic studies for SCLC (18). Information regarding age, sex, ethnicity, pathologic TNM stage (the 7th classification), and smoking status was collected retrospectively (Supplementary Tables S1 and S4).

Copy number analysis

Copy-number alterations in cohort 1 were examined by quantitative real-time PCR. Genomic DNA was extracted using a QIAamp DNA mini kit (QIAGEN) in accordance with the manufacturer's instructions. Quantitative real-time PCR (qRT-PCR) was performed using a TaqMan copy number assay (Thermo Fisher Scientific) and the 7900 HT Fast Real-Time PCR System (Thermo Fisher Scientific). DNA (10 ng) was added to each 10 μ L

PCR reaction, which contained TaqMan Universal Genotyping Master Mix. All assays were performed in quadruplicate and investigators were blinded to the clinical outcome. The following TaqMan probes were purchased from Thermo Fisher Scientific: *CD274* (Assay ID: Hs00268713_cn), *PDCD1LG2* (Hs01115641_cn), *JAK2* (Hs02831068_cn), *PLGRKT* (Hs03723314_cn), *KIAA1432* (Hs03076906_cn), *FLJ41200* (Hs03718447_cn), and *NFIB* (Hs01324052_cn). RNase P (#4403326) was used as a reference control. The predicted copy number was calculated using CopyCaller v2.0 (Thermo Fisher Scientific) and normalized to the mean of noncancerous tissues from ten Japanese individuals in this study. Samples from cohort 1 were further analyzed with human 250K Nsp SNP arrays, followed by data processing using Copy Number Analyzer for Affymetrix GeneChip Mapping Array (CNAG) software, ver.2.0 (17). Copy number was determined with respect to the copy number of noncancerous lung tissues of the same patient. In addition, cases from cohort 1 ($n = 10$) were analyzed by SNP 6.0 array following the procedure as previously described (18).

Copy number alterations of samples from cohort 2 ($n = 138$) were calculated from Affymetrix Genome-Wide Human SNP array 6.0 data ($n = 132$) or by referring to copy-number data calculated from whole-genome sequencing ($n = 98$). The data were analyzed as previously described (18). Genomic regions are determined according to the human reference genome NCBI37/hg19.

GISTIC 2.0 was used to determine significant copy number alterations for the SNP 6.0 Array data from samples of cohort 1 and 2 (19). Genomic regions with a \log_2 ratio of above 0.5 were considered as amplified. The significance threshold was set at $Q = 0.25$.

Whole-genome and transcriptome sequencing analysis

Whole-genome sequencing was performed as previously described (18). Genomic copy numbers were deduced from the number of sequence reads and described as integral copy number (iCN) values. Transcriptome sequencing data of cohort 1 ($n = 7$; ref. 17) and cohort 2 ($n = 74$; ref. 18) were analyzed following the computational approach as described previously (18). The transcript levels of each gene were analyzed as FPKM (Fragments Per Kilobase of transcript per Million mapped reads) values. The transcriptome sequencing data were used to analyze for transcripts specific for B cells (*CD19*) and T cells (*CD3E*), and to further define T-cell subsets for CD8 T cells (average of *CD8A* and *CD8B* transcripts), CD4 T cells (*CD4*) and regulatory T cells (Tregs, average of *FOXP3* and *IL2RA* transcripts).

Immunohistochemistry

Tissue block sections (4- μ m thick) were deparaffinized, incubated in xylene and ethanol, and then washed with water. For antigen retrieval, sections were boiled in 10 mmol/L sodium citrate buffer for 10 minutes at 121°C, rinsed with water, incubated in 3% peroxidase, and then washed with water followed by buffer. For PD-L1 staining, sections were incubated with anti-PD-L1 (E1L3N; Cell Signaling Technology) diluted 1:800 with antibody diluent (Signal Stain Antibody Diluent #8112, Cell Signaling Technology), followed by a peroxidase-labeled secondary antibody (EnVision/HRP System; DAKO), rinsed in buffer, and immersed in DAB substrate. IHC of a Cohort 2 sample showing focal *CD274* amplification was performed as previously

described (14). FFPE sections were stained for SCLC marker: CD56 (clone 123C3, dilution: 1:500, Zytomed), synaptophysin (clone SP11, dilution: 1:50, Thermo Fisher Scientific), chromogranin A (clone DAK-A3, dilution 1:500; Dako Cytomation), and Ki-67 (clone SP6, dilution: 1:100, Cellmarque). The following immune cell markers were used for IHC: CD3 (clone SP7, dilution: 1:50, Thermo Fisher Scientific), CD4 (clone 4B12, dilution: 1:100, Thermo Fisher Scientific), CD8A (clone C8/144B, dilution: 1:200, Dako) and CD20 (clone L26, dilution: 1:1250, Dako).

Immunostaining for PD-L1 was evaluated by at least two independent observers (M. Saito, K. Tsuta, and A.H. Scheel) using the H-score method, as previously described (20). Briefly, staining percentages (0%–100%) and the intensity (0, negative; 1, very weak expression; 2, moderate expression; 3, strong expression) in tumor cells were evaluated and then immunostained slides were scored ranging from 0 to 300 by multiplying the percentage of tumor area. For PD-L1 expression, a score of 3 was used as the cut-off score due to the antibody specificity.

Results

We first sought for mutations affecting the *CD274* gene in four SCLC sequencing studies; however, no recurrent mutations were found (18, 21–23). We then examined in detail changes in the chromosomal copy number of the *CD274* (PD-L1) locus in two cohorts of SCLC tumors. We had previously observed copy number gains of 9p24, in which *CD274* resides (17) and thus performed genomic quantitative PCR in a larger cohort (54 primary SCLC tumors and 34 metastases) obtained from 72 patients (Table 1 and Supplementary Table S2). In addition to *CD274*, we also examined the copy number states of representative cancer-related genes that mapped telomeric and centromeric to *CD274*, such as *NFIB* and *FLJ41200* at 9p23 and *KIAA1432*, *PDCD1LG2*, *PLGRKT*, and *JAK2* at 9p24.1 (Fig. 1A). *NFIB* and *JAK2* have been suggested to play a role in lung cancer and were therefore included in this analysis (24, 25). Three tumors showed an increase in somatic *CD274* copy number (≥ 4 ; Fig. 1A, Sup-

plementary Fig. S1, Supplementary Table S3), and two of these (9-P/SM09-010T and 38-P/R-513T) exhibited focal and high-level amplification (copy numbers, 39.9 and 5.7, respectively) of the segment containing the *CD274* gene and of the neighboring genes, *KIAA1432* and *PDCD1LG2*, the latter of which encodes the PD-L2 protein. Tumor specimen 6-P/SM09-006T exhibited polysomy of chromosome 9p (Fig. 1A, Supplementary Fig. S1). These findings were confirmed by analyzing SNP array data that revealed focal, high-level amplification of the locus comprising *CD274* (Fig. 1B) in case 9-P and 38-P, but not in the polysomic case, 6-P (Supplementary Fig. S1). In the cases, 9-P and 38-P, amplification occurred on one allele within the chromosome 9p24 segment (17), as evidenced by analyses of allele-specific copy number (Supplementary Fig. S1).

Tumor specimens from cohort 2 (135 primary lung tumors and three metastatic tumors; Table 1 and Supplementary Table S2) were analyzed by SNP 6.0 arrays and whole genome sequencing (18), which revealed focal amplification of *CD274* in four cases (Fig. 1C), of which two tumors had copy numbers greater than four (case S00213 and S02404, Fig. 1D and Supplementary Table S3). Detailed analyses of the copy number gain affecting the 9p24 locus revealed that the minimally amplified region included *CD274* and the neighboring genes, *PDCD1LG2* and *KIAA1432* (Fig. 1B and D). SNP 6.0 array data that was available for samples from both cohorts (refs. 17, 18; Supplementary Table S3), and the combined analysis further pointed to a significant and focal amplification of the 9p24 locus harboring *CD274* (Q -value = 0.11, Supplementary Fig. S2A). SCLC tumor cases with significant *CD274* amplifications showed the same level of genomic amplification across the genome as observed in other SCLC cases with amplified genomic regions ($P = 0.21$, Supplementary Fig. S2B). In summary, four SCLC tumors from two cohorts (4/210, 1.9%) exhibited focal and high-level amplification of *CD274* and the neighboring *PDCD1LG2* and *KIAA1432* genes. Of note, three of these four cases were of Asian ethnicity. However, these four SCLC patients had no clinical or pathological features discriminating them from other cases (Supplementary Tables S1 and S4).

By analyzing whole-genome sequencing data, we observed multiple intra- and interchromosomal rearrangements in case 9-P (cohort 1) and case S02404 (cohort 2), which affected the 9p24.1 segment (Fig. 2A, Supplementary Fig. S3, and Supplementary Table S5). Of note, a genomic rearrangement occurred in the upstream promoter and 5'-UTR region of *CD274*. This led to a tandem duplication of the region upstream of *CD274* in case 9-P, compatible with amplification of *CD274* enhancer elements (26). Case S02404, on the contrary, revealed intra- and interchromosomal rearrangements, which involved a series of amplification patterns causing the observed *CD274* amplification. However, the copy number state within the genomic segment encoding the *CD274* open reading frame was not altered (Fig. 2A). This finding raises the possibility that genomic rearrangements in the 9p24 locus upstream of *CD274* may result in deregulation of *CD274* expression, without altering the coding region.

We therefore analyzed transcriptome sequencing data from these tumors, which revealed high expression of the *CD274* transcript in cases with high-level focal amplification of *CD274* (Supplementary Table S3, Supplementary Table S6). Of note, amplification of 9p24 also resulted in higher expression of other genes contained in the amplified locus (Supplementary Fig. S4A, Supplementary Table S6). However, of the genes in the minimally amplified region, *CD274* was the most highly expressed in case

Table 1. Patient characteristics in two study cohorts

	Cohort 1 (n = 72)	Cohort 2 (n = 138)
Age, y		
Mean (range)	65.1 (47–89)	64 (33–83)
Sex number (%)		
Male	56 (78)	83 (60)
Female	16 (22)	55 (40)
Ethnicity (%)		
Asian	66 (92)	7 (5)
Caucasian	2 (3)	63 (46)
African American	4 (5)	0
Unknown	0	68 (49)
Smoking (pack year) number (%)		
Never smoker	5 (7)	1 (0.7)
Current smoker	—	68 (49.3)
Former smoker	—	43 (31.2)
<20	3 (4)	—
≥ 20	55 (76)	—
Unknown	9 (13)	26 (18.8)
TNM stage (%)		
I	20 (28)	42 (30.4)
II	11 (15)	25 (18.1)
III	19 (26)	32 (23.2)
IV	22 (31)	31 (22.5)
N/A	0	8 (5.8)

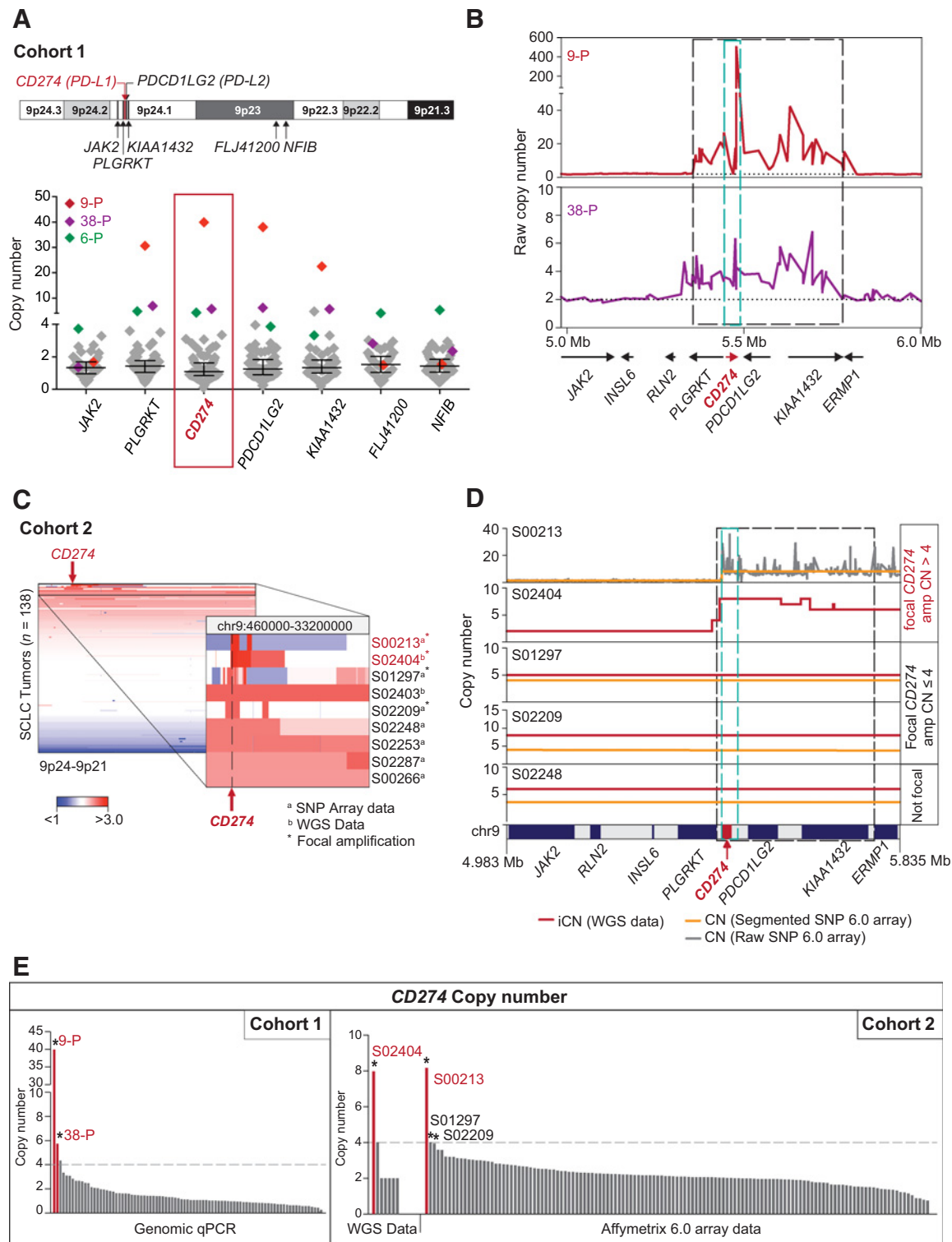


Figure 1. Focal amplification of *CD274* in small-cell lung carcinoma (SCLC). **A**, Schematic representation of the 9p locus encompassing *CD274* (top). The highlighted genes were subjected to quantitative real-time genomic PCR analysis in cohort 1 samples (bottom). **B**, Raw copy numbers of the 9p24 locus derived from 250 K Affymetrix SNP array data were plotted for tumors 9-P and 38-P. Dashed black lines indicate the minimally amplified region for cohort 1 samples. Dashed blue lines point to the *CD274* locus. **C**, Copy number analysis of cohort 2 samples based on Affymetrix SNP 6.0 and whole-genome sequencing (WGS) data. Shown are normalized and segmented copy number data of the tumors with the highest 9p24 copy number. Tumors are sorted according to copy number. **D**, Detailed representation of the copy number states in cohort 2 samples with 9p24 amplification. Dashed black lines indicate the minimally amplified region for cohort 2 samples. Dashed blue lines point to the *CD274* locus. **E**, Bar plot displaying the copy number state for *CD274* in cohort 1 and 2. *, cases with focal 9p24 amplifications.

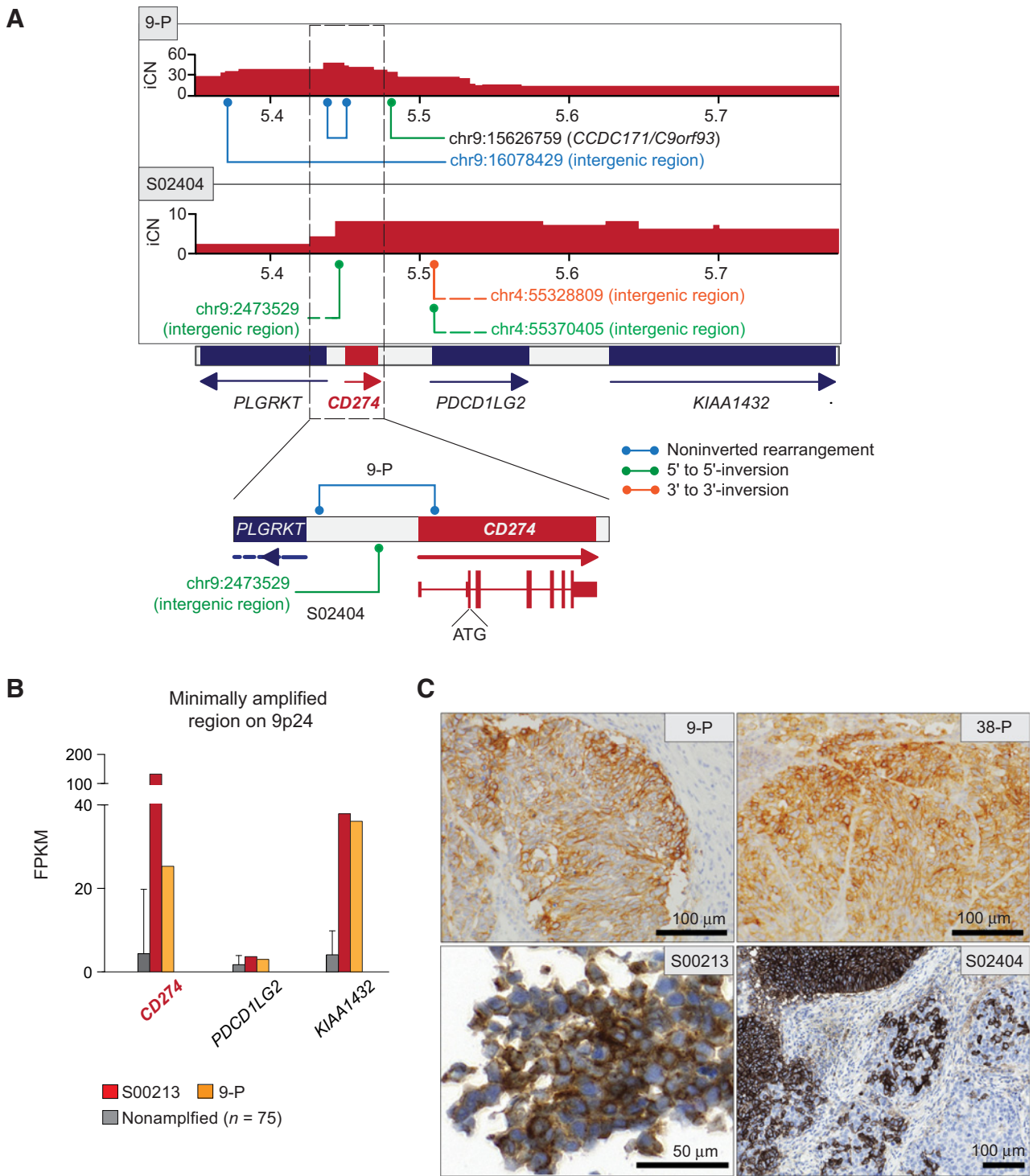


Figure 2. High-level PD-L1 expression in SCLC tumors with high-level focal amplification of *CD274*. **A**, Copy number states and genomic rearrangements determined by whole-genome sequencing for cases 9-P and S02404. The 9p24 locus encompassing the genes *PLGRKT*, *CD274*, *PDCD1LG2*, and *KIAA1432* is displayed. Copy numbers are plotted as integral copy numbers (iCN), and genomic breaks leading to genomic rearrangements are annotated below the graph as noninverted rearrangements (blue) or inversions (5'-to-5' as green, 3'-to-3' as orange). Dashed black lines highlight the chromosomal locus of *CD274*. Exon regions in *CD274* are represented as boxes (small boxes: noncoding exons, large boxes: coding exons). **B**, Expression of genes located in the minimally amplified region of the 9p24.1 amplicon, expressed as FPKM values. Case 9-P and S00213 were compared with 75 nonamplified cases (mean+SD). **C**, Immunohistochemistry for PD-L1 protein expression in 9p24-amplified SCLC tumors. Scale bar as indicated.

Downloaded from <http://aacrjournals.org/clincancerres/article-pdf/23/5/1220/1930725/1220.pdf> by guest on 17 April 2025

9-P and one of the two most highly expressed in case S00213 (Fig. 2B). Thus, *CD274* appears to be the target of the 9p24 amplification.

We next examined whether high-level focal *CD274* amplification and high transcript levels were associated with PD-L1 protein expression. We therefore performed immunohistochemical analyses of PD-L1 protein expression using the PD-L1 antibody E1L3N. The specificity of this antibody has been validated in knockdown studies and has been used in several studies examining PD-L1 expression (20, 27, 28), including SCLC (14). We studied tumors bearing focal *CD274* amplification and 15 additional tumors from cohort 1, including the 9p-polysomic case. Only the four focally amplified cases contained tumor cells that stained positive for PD-L1 while confirming the classic SCLC morphology (Supplementary Fig. S4B); all other tumors, including 9p-polysomic case, were PD-L1-negative (Fig. 2C, Supplementary Fig. S4C, and Supplementary Table S7). We additionally quantified the level of immune cell infiltrates based on transcriptome sequencing data. PD-L1 expression positively correlated with infiltration of immune cells, as determined by expression of markers specific for B cells and T-cell subsets (Supplementary Fig. S5A). Tumors bearing *CD274* amplification ranged among those SCLC tumor cases which showed elevated transcript levels for immune cell markers, which was further confirmed by IHC (Supplementary Fig. S5B). These results suggest that focal *CD274* amplification is associated with high PD-L1 antigen expression.

Discussion

Here, we report that a subset (2%) of SCLC bear focal and high-level amplification of *CD274* resulting in high expression of PD-L1. By contrast, tumors with nonfocal, low-amplitude copy number gain of 9p24 (where *CD274* resides), or tumors lacking gain or amplification of 9p24, did not exhibit high expression of PD-L1. These findings suggest that genomic upregulation of the *CD274* gene is possibly a mechanism for immune evasion in SCLC and thus such tumors might be particularly vulnerable to immune checkpoint inhibition.

Recent studies emphasized the role of focal gene amplifications in activation of proto-oncogenes in various cancers (29–34), and a genomic study across 22 major cancer types, which does not include SCLC, found that *CD274* was amplified in 12% of the cases (35). Focal amplification of the *MYCL1*, *MYCN*, and *MYC* oncogenes are known genomic events in SCLC (36). Our findings suggest that amplification of *CD274* may be yet another mechanism during oncogenic transformation providing a specific route to immune evasion. Of the other genes that are contained in the focal 9p24 amplicon, only *CD274*, *PDCD1LG2*, and *KIAA1432* genes are in the minimally amplified region. Of note, co-amplification of the neighboring gene *PDCD1LG2*, encoding another PD-1 ligand, PD-L2, did not lead to strong upregulation of corresponding PD-L2 transcript levels as observed for *CD274* (Fig. 2D). Therefore, PD-L1, rather than PD-L2, seems to play a major role in suppressing immune responses in 9p24 amplified SCLC tumors.

References

1. Govindan R, Page N, Morgensztern D, Read W, Tierney R, Vlahiotis A, et al. Changing epidemiology of small-cell lung cancer in the United States over

In summary, our results provide evidence for genomic upregulation of PD-L1 expression in a subset of SCLC. We speculate that SCLC tumors with amplification of *CD274* may be particularly sensitive to therapeutic PD-1/ PD-L1 inhibition.

Disclosure of Potential Conflicts of Interest

R. Nishikawa reports receiving speakers bureau honoraria from Astaris, Chugai, Eisai, MSD, Nobel Pharma, Novocure, Ohtsuka, and Ohno. M. Peifer is a consultant/advisory board member for NEO New Oncology GmbH. I. Petersen is a consultant/advisory board member for Bristol-Myers Squibb, MSD, and Roche. R.K. Thomas is a consultant/advisory board member for Clovis, Johnson & Johnson, New Oncology AG, and Roche. No potential conflicts of interest were disclosed by the other authors.

Authors' Contributions

Conception and design: J. George, M. Saito, R. Büttner, J. Yokota, R.K. Thomas, T. Kohno

Development of methodology: J. George, K. Tsuta, M. Peifer, R.K. Thomas
Acquisition of data (provided animals, acquired and managed patients, provided facilities, etc.): J. George, K. Tsuta, K. Shiraishi, A.H. Scheel, S. Uchida, S. Watanabe, R. Nishikawa, M. Noguchi, S.J. Jang, R. Büttner, C.C. Harris, J. Yokota

Analysis and interpretation of data (e.g., statistical analysis, biostatistics, computational analysis): J. George, M. Saito, R. Iwakawa, A.H. Scheel, R.K. Thomas

Writing, review, and/or revision of the manuscript: J. George, M. Saito, K. Tsuta, R. Iwakawa, A.H. Scheel, M. Peifer, S.J. Jang, C.C. Harris, R.K. Thomas, T. Kohno

Administrative, technical, or material support (i.e., reporting or organizing data, constructing databases): S.J. Jang, I. Petersen, R. Büttner, J. Yokota
Study supervision: J. George, R.K. Thomas

Acknowledgments

We thank Drs. Akiteru Goto and Masayuki Tsuneki for support and comments.

Grant Support

This work was supported by Grants-in-Aid from the Japan Agency for Medical Research and Development (AMED: 16ck0106012h0003) and a Grant-in-Aid from the Japanese Society for the Promotion of Science (JSPS) and Scientific Research (B: 26293200). NCC Biobank was supported by the National Cancer Center Research and Development Fund (26A-1). C C Harris was supported by intermural funding from the National Cancer Institute, NIH. This work was also supported by the German Cancer Aid (Deutsche Krebshilfe) as part of the small-cell lung cancer genome sequencing consortium (grant ID: 109679; to R.K. Thomas, R. Büttner, and M. Peifer), by the German Ministry of Science and Education (BMBF) as part of the e:Med program (grant no. 01ZX1303A; to R.K. Thomas, R. Büttner, and M. Peifer), by the Deutsche Forschungsgemeinschaft (DFG; through TH1386/3-1 to R.K. Thomas), by the Deutsche Krebshilfe as part of the Oncology Centers of Excellence funding program (to R.K. Thomas) and by the German Cancer Consortium (DKTK) Joint Funding program.

The costs of publication of this article were defrayed in part by the payment of page charges. This article must therefore be hereby marked *advertisement* in accordance with 18 U.S.C. Section 1734 solely to indicate this fact.

Received April 27, 2016; revised July 30, 2016; accepted August 23, 2016; published OnlineFirst September 12, 2016.

the last 30 years: analysis of the surveillance, epidemiologic, and end results database. *J Clin Oncol* 2006;24:4539–44.

2. William WN Jr, Glisson BS. Novel strategies for the treatment of small-cell lung carcinoma. *Nat Rev Clin Oncol* 2011;8:611–9.
3. Tumei PC, Harview CL, Yearley JH, Shintaku IP, Taylor EJ, Robert L, et al. PD-1 blockade induces responses by inhibiting adaptive immune resistance. *Nature* 2014;515:568–71.
4. Postow MA, Callahan MK, Wolchok JD. Immune checkpoint blockade in cancer therapy. *J Clin Oncol* 2015;33:1974–82.
5. Ansell SM, Lesokhin AM, Borrello I, Halwani A, Scott EC, Gutierrez M, et al. PD-1 blockade with nivolumab in relapsed or refractory Hodgkin's lymphoma. *N Engl J Med* 2015;372:311–9.
6. Brahmer JR, Tykodi SS, Chow LQ, Hwu WJ, Topalian SL, Hwu P, et al. Safety and activity of anti-PD-L1 antibody in patients with advanced cancer. *N Engl J Med* 2012;366:2455–65.
7. Topalian SL, Hodi FS, Brahmer JR, Gettinger SN, Smith DC, McDermott DF, et al. Safety, activity, and immune correlates of anti-PD-1 antibody in cancer. *N Engl J Med* 2012;366:2443–54.
8. Garon EB, Rizvi NA, Hui R, Leigh N, Balmanoukian AS, Eder JP, et al. Pembrolizumab for the treatment of non-small-cell lung cancer. *N Engl J Med* 2015;372:2018–28.
9. Calvo E, Lopez-Martin JA, Bendell J, Eder JP, Taylor M, Ott PA, et al. Nivolumab (NIVO) monotherapy or in combination with ipilimumab (IPI) for treatment of recurrent small cell lung cancer (SCLC). *Eur J Cancer* 2015;51:S633–S.
10. Ott PA, Fernandez MEE, Hirt S, Kim DW, Moss RA, Winser T, et al. Pembrolizumab (MK-3475) in patients (pts) with extensive-stage small cell lung cancer (SCLC): preliminary safety and efficacy results from KEYNOTE-028. *J Clin Oncol* 33, 2015 (suppl; abstr 7502).
11. Topalian SL, Drake CG, Pardoll DM. Immune checkpoint blockade: a common denominator approach to cancer therapy. *Cancer Cell* 2015;27:450–61.
12. Taube JM, Klein A, Brahmer JR, Xu H, Pan X, Kim JH, et al. Association of PD-1, PD-1 ligands, and other features of the tumor immune microenvironment with response to anti-PD-1 therapy. *Clin Cancer Res* 2014;20:5064–74.
13. Rizvi NA, Hellmann MD, Snyder A, Kvistborg P, Makarov V, Havel JJ, et al. Cancer immunology. Mutational landscape determines sensitivity to PD-1 blockade in non-small cell lung cancer. *Science* 2015;348:124–8.
14. Schultheis AM, Scheel AH, Ozretic L, George J, Thomas RK, Hagemann T, et al. PD-L1 expression in small cell neuroendocrine carcinomas. *Eur J Cancer* 2015;51:421–6.
15. Ishii H, Azuma K, Kawahara A, Yamada K, Imamura Y, Tokito T, et al. Significance of programmed cell death-ligand 1 expression and its association with survival in patients with small cell lung cancer. *J Thorac Oncol* 2015;10:426–30.
16. Komiya T, Madan R. PD-L1 expression in small cell lung cancer. *Eur J Cancer* 2015;51:1853–5.
17. Iwakawa R, Takenaka M, Kohno T, Shimada Y, Totoki Y, Shibata T, et al. Genome-wide identification of genes with amplification and/or fusion in small cell lung cancer. *Genes Chromosomes Cancer* 2013;52:802–16.
18. George J, Lim JS, Jang SJ, Cun Y, Ozretic L, Kong G, et al. Comprehensive genomic profiles of small cell lung cancer. *Nature* 2015;524:47–53.
19. Mermel CH, Schumacher SE, Hill B, Meyerson ML, Beroukhi R, Getz G. GISTIC2.0 facilitates sensitive and confident localization of the targets of focal somatic copy-number alteration in human cancers. *Genome Biol* 2011;12:R41.
20. Katsuya Y, Fujita Y, Horinouchi H, Ohe Y, Watanabe S, Tsuta K. Immunohistochemical status of PD-L1 in thymoma and thymic carcinoma. *Lung Cancer* 2015;88:154–9.
21. Peifer M, Fernandez-Cuesta L, Sos ML, George J, Seidel D, Kasper LH, et al. Integrative genome analyses identify key somatic driver mutations of small-cell lung cancer. *Nat Genet* 2012;44:1104–10.
22. Rudin CM, Durinck S, Stawiski EW, Poirier JT, Modrusan Z, Shames DS, et al. Comprehensive genomic analysis identifies SOX2 as a frequently amplified gene in small-cell lung cancer. *Nat Genet* 2012;44:1111–6.
23. Iwakawa R, Kohno T, Totoki Y, Shibata T, Tsuchihara K, Mimaki S, et al. Expression and clinical significance of genes frequently mutated in small cell lung cancers defined by whole exome/RNA sequencing. *Carcinogenesis* 2015;36:616–21.
24. Dooley AL, Winslow MM, Chiang DY, Banerji S, Stransky N, Dayton TL, et al. Nuclear factor I/B is an oncogene in small cell lung cancer. *Genes Dev* 2011;25:1470–5.
25. Lipson D, Capelletti M, Yelensky R, Otto G, Parker A, Jarosz M, et al. Identification of new ALK and RET gene fusions from colorectal and lung cancer biopsies. *Nat Med* 2012;18:382–4.
26. Huang G, Wen Q, Zhao Y, Gao Q, Bai Y. NF-kappaB plays a key role in inducing CD274 expression in human monocytes after lipopolysaccharide treatment. *PLoS One* 2013;8:e61602.
27. Twyman-Saints Victor C, Rech AJ, Maity A, Rengan R, Pauken KE, Stelekati E, et al. Radiation and dual checkpoint blockade activate non-redundant immune mechanisms in cancer. *Nature* 2015;520:373–7.
28. Wimberly H, Brown JR, Schalper K, Haack H, Silver MR, Nixon C, et al. PD-L1 expression correlates with tumor-infiltrating lymphocytes and response to neoadjuvant chemotherapy in breast cancer. *Cancer Immunol Res* 2015;3:326–32.
29. Cancer Genome Atlas Research Network. Comprehensive molecular profiling of lung adenocarcinoma. *Nature* 2014;511:543–50.
30. Cancer Genome Atlas Research Network. Comprehensive genomic characterization of squamous cell lung cancers. *Nature* 2012;489:519–25.
31. Cancer Genome Atlas Research Network. Comprehensive molecular characterization of clear cell renal cell carcinoma. *Nature* 2013;499:43–9.
32. Cancer Genome Atlas Research Network, Kandoth C, Schultz N, Cherniack AD, Akbani R, Liu Y, et al. Integrated genomic characterization of endometrial carcinoma. *Nature* 2013;497:67–73.
33. Cancer Genome Atlas Research Network. Comprehensive molecular characterization of gastric adenocarcinoma. *Nature* 2014;513:202–9.
34. Cancer Genome Atlas Network. Comprehensive molecular portraits of human breast tumours. *Nature* 2012;490:61–70.
35. Budczies J, Bockmayr M, Denkert C, Klauschen F, Groschel S, Darb-Esfahani S, et al. Pan-cancer analysis of copy number changes in programmed death-ligand 1 (PD-L1, CD274) - associations with gene expression, mutational load, and survival. *Genes Chromosomes Cancer* 2016;55:626–39.
36. Wistuba II, Gazdar AF, Minna JD. Molecular genetics of small cell lung carcinoma. *Semin Oncol* 2001;28:3–13.